2018 EAGE ANNUAL
80TH CONFERENCE + EXHIBITION
COPENHAGEN | DENMARK

Th C 06

De-noising Strategy on Single-source Single-sensor Data: a Case Study from North Kuwait

T. Rebert* (CGG), J. Rivault (CGG), G. Gigou (CGG), L. Vivin (CGG), H. Toubiana (CGG), S. Baillon (CGG), A. Prescott (CGG), D. Le Meur (CGG), A. El-Emam (KOC), H. Bayri (KOC)

Summary

This paper reviews the benefits of using “high-end new-generation” de-noising tools on a broadband single-source single-sensor Wide Azimuth survey from North Kuwait. The survey was acquired in a very challenging area containing agricultural and industrial zones, as well as various natural and man-made obstructions, leading to large holes and irregularities in the acquisition. We demonstrate that the chosen solution correctly recovers the broadband signal, by applying optimum processing on highly noise contaminated data. Once properly de-noised, a 5D interpolation process was used to reconstruct a high resolution image, from the shallow to the deeper section. Appropriate de-noising sequence prior to the 5D interpolation was crucial for further processing steps such as multiple attenuation, pre-stack time and depth imaging and reservoir characterization.

Introduction

The use of broadband high density land acquisition has increased in recent years due to the benefits it can offer for de-aliasing noise and producing high resolution images (Le Meur et al., 2013). While conventional acquisition reduces pre-stack noise levels by deploying source and receiver arrays, modern high density acquisitions typically deploy single-source single-sensor configurations, increasing trace density, but at the cost of pre-stack signal-to-noise ratio. This paper reviews the benefits of a de-noising sequence applied to a broadband single-source single-sensor (S^4) Wide Azimuth (WAZ) dataset acquired in North Kuwait. The objective of the project was to improve seismic data quality and preserve broadband signal for structural imaging and calibrated stratigraphic inversion. This 100 000 channel survey was acquired with an orthogonal geometry, having a source and receiver line spacing of 200 m, and a maximum offset of 6000 m in both inline and crossline directions (El-Emam and Saaba, 2015). For each shot line, the shot point interval was 25 m and each receiver line consisted of 4 sub-lines of point receivers arranged in a staggered pattern (Figure 1d). The survey area has several obstacles including agricultural and industrial areas, dwellings and roads leading to a highly irregularly sampled dataset with empty or low fold areas with irregular offset and azimuth distributions (Figure 1a-b). Despite a weak signal-to-noise ratio on each elementary trace, the noise content was sufficiently spatially de-aliased to perform efficient de-noising. A geophone summation was performed to reduce the receiver sampling to 25 m (Figure 1c) following which surface-consistent processing, residual de-noising, and 5D interpolation were applied. This paper illustrates the benefits of this "high-end new-generation" de-noising workflow in recovering the original characteristics of the wavelet for properly rebuilding parts of the pilot that were poorly covered during the acquisition.

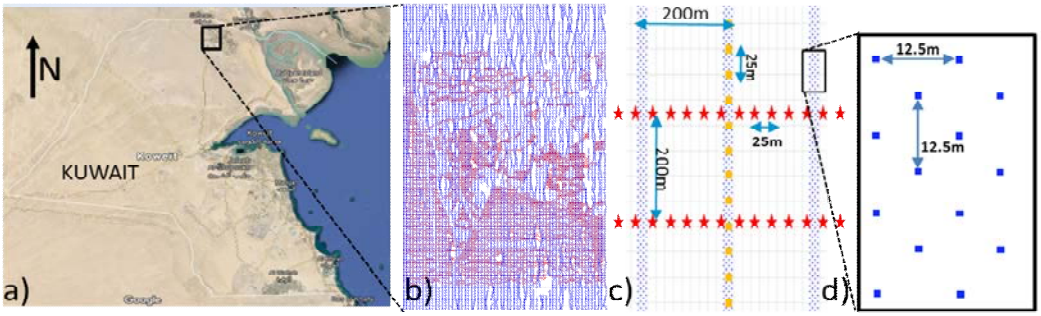

Figure 1 *a) 150 km^2 pilot area in North Kuwait (black rectangle), b) basemap where shots and receivers are drawn in red and blue respectively, c) acquisition design where single-source (red) single-receiver (blue) positions are overlaid by the receiver positions after the Digital Array Forming (orange square), and d) zoom of staggered receiver positions inside each receiver line.*

Noise attenuation of single-source-single sensor

Pre-stack S^4 data are inherently noisier than vintage data acquired with large field arrays acting as a strong noise filter. The source of the noise can be categorized into three classes: acquisition-related (vibrators, sweep harmonics, instrumental), undesired propagating waves (air waves, surface waves, guided waves, back-scattering, internal multiples) and environmental noise (wind, industrial activity). A sequential workflow was devised to tackle each of these noise classes which was applied to the raw data (Figure 2a), resulting in de-noised data (Figure 2b). Although all these types of noise were strongly attenuated, the real challenge was to preserve the underlying weak broadband signal (Figure 2b). The only way to achieve signal preservation was to apply noise attenuation in the recorded data domain where the distance between each source and receiver was minimal (here 12.5 m between receivers and 25 m between sources). In this case, the surface waves were less aliased which made them easier to model and remove. Firstly, high amplitude spikes and erratic noise were removed using a joint low-rank and sparse inversion method (Sternfels et al., 2015). The air-wave appeared linear in the cross-spread domain and was parameterised using a model with a velocity range between 340 m/s and 360 m/s and a frequency range from 40 Hz to 110 Hz. In a second step, this air-wave model was adaptively subtracted from the raw data (Figures 2 a-b, green arrow). The third step concerned the

surface wave attenuation where two types of model were built, the first one using a data-driven interferometry approach (Chiffot et al., 2017), the second one using an adaptive modelling (Le Meur et al., 2008). The data-driven interferometry provided better modelling of the surface wave apices on broadside cables but required regularization and densification of the cross-spread. This was achieved using interpolation (down to 6.25 m in both directions) by joint low-rank and sparse inversion (Sternfels et al., 2016) which fully de-aliased the surface waves. The use of adaptive modelling allowed for better handling of the surface and guided waves at the nearest offsets. The de-noised result is shown on a cross-spread (Figure 2 a-b).

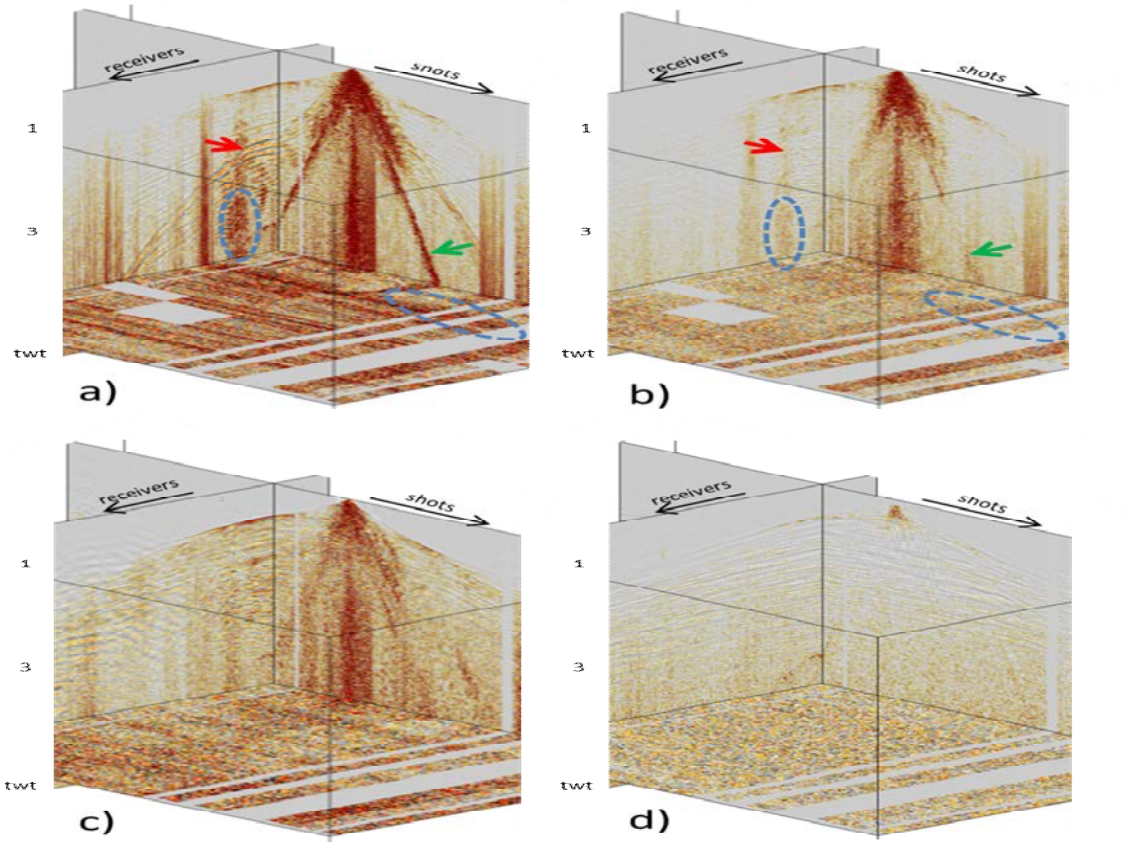

Figure 2 *a) 3D view of a single S^4 cross-spread before de-noising. Random noise (dashed blue circle), air-wave (green arrow) and surface waves (red arrow) are clearly visible, b) after de-noising, c) after digital array forming (DAF), and d) after surface-consistent processing and additional de-noising.*

Processing after Digital Array Forming and 5D regularization

The intra-array statics were computed after successful removal of large part of coherent and random noise. This was followed by Digital Array Forming (DAF) on the receiver side in order to produce new receiver positions every 25 m (Figure 1c). After the DAF, the sequence was similar to conventional WAZ survey processing (Figure 2c). The sweep for the acquisition was broadband (2–84 Hz), therefore inverse geophone response filter was applied to recover signal at the very low frequencies (2-8 Hz). All surface-consistent attributes (amplitude and residual statics) and operators (deconvolution and phase) were derived using WAZ compliant algorithms (Poulain et al., 2014). Horizontal and vertical amplitude stripes were balanced by applying surface-consistent processing in octaves, resulting in the data illustrated in Figure 2d. Finally, a pass of linear noise attenuation was applied in the cross-spread domain to address residual guided waves. Stack and octave panels after the de-noising and the surface-consistent processing show a better preservation of the broadband signal where horizons appeared more continuous and sharper (Figure 3a-b). The weak signal embedded within a high noise level was well-recovered especially on the lower octaves (2-8 Hz) (Figure 3 c-d). 5D data reconstruction was used to generate traces on a theoretical regular geometry using an anti-leakage Fourier transform (Poole, 2010). In order to reconstruct the data in the shallow part and fill

the large holes due to the irregular acquisition, denser shot and receiver lines were created every 100 m. In this particular case, the process allowed an interpolation of a large part of the missing near offsets (Figure 4a). The migrated section shows a clear uplift after 5D regularization, large holes were reduced (green circles and arrows), the signal to noise ratio and the continuity of the horizon were improved and the acquisition footprint was reduced (Figure 4b). The comparison with the vintage data shows that a dedicated effective de-noising, which better preserved the broadband signal, was key to reconstructing the shallow part of the data with a 5D algorithm (Figure 4).

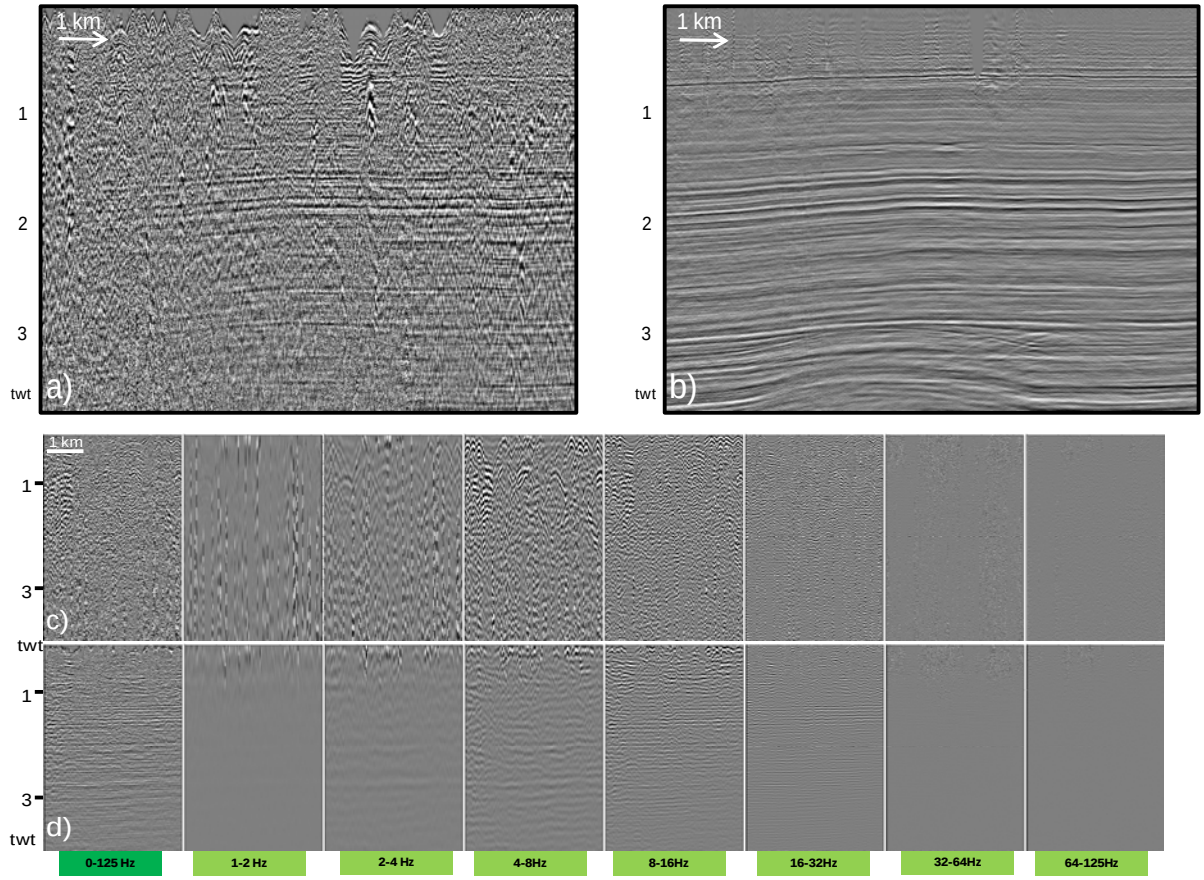

Figure 3 *a) Stack before de-noising, b) stack after surface consistent processing and additional de-noising, c) octave panels before de-noising, and d) octave panels after the de-noising.*

Conclusions

The fit-for-purpose tested and applied approach has demonstrated the benefits in handling high-density broadband single-source single-sensor data on a highly irregularly spatially sampled Wide-Azimuth dataset. Such modern acquisition can provide a very high-resolution image when methods such as joint low-rank and sparse inversion combined with surface wave interferometry are used to recover broadband signal on highly noise contaminated elementary traces. Processing high density surveys requires efficient surface-consistent approaches to ensure consistency and reliability to recover broadband signal from the shallowest to the deepest part prior to 5D interpolation. The de-noising will ease further processing steps such as multiple attenuation, pre-stack time and depth imaging and reservoir characterization.

Acknowledgements

We are grateful to the Kuwait Oil Company for the permission to present this data example. We also thank CGG for permission to publish our results.

References

El-Emam, A. and El Sabaa, A. [2015] Quantitative Analysis of Point Receiver 3D Seismic for Optimum and Cost Effective Survey Design, Case Study. *77th Annual international conference and exhibition, EAGE*, Expanded abstracts.

Chiffot, C., Prescott, A., Grimshaw, M., Oggioni, F., Kowalczyk-Kedzierska, M., Cooper, C., Johnston, R.G. [2017] Data-driven interferometry method to remove spatially aliased and non-linear surface waves. *87th Annual International Meeting, SEG*, Expanded Abstracts.
Le Meur, D., Benjamin, N., Cole, R. and Harthy, M. [2008] Adaptive groundroll filtering. *77th Annual international conference and exhibition, EAGE*, Expanded abstracts.
Le Meur, D., Herrmann, P., Leveque, A., Baillon, S., Duwattez, X., Suaudeau, E., Poulain, G., Garceran, K. [2013] Challenges on Ultra High-Density Seimic Survey: Array Free Processing. *75th Annual international conference and exhibition, EAGE*, Expanded abstracts.
Poulain. G., Garceran, K., Grimshaw, M., Le Meur, D., Murray, E., Kowalczyk, M., Cooper, S., Ourabah, A. [2014] Surface-Consistent Processing of a full-azimuth dataset: the challenges and solutions. *76th Annual international conference and exhibition, EAGE*, Expanded abstracts.
Poole, G. [2010] 5D data reconstruction using the anti-leakage Fourier transform. Adaptive groundroll filtering. *72nd Annual international conference and exhibition, EAGE*, Expanded abstracts.
Sternfels, R., Prescott, A., Pignot, G., Tian, L. and Le Meur, D. [2016] Irregular spatial sampling and rank reduction: interpolation by joint low-rank and sparse inversion. *78th Annual international conference and exhibition, EAGE*, Expanded abstracts.
Sternfels, R., Viguier, G., Gondoin, R. and Le Meur, D. [2015] Multidimensional simultaneous random plus erratic noise attenuation and interpolation for seismic data by Joint Low-Rank and Sparse Inversion. *Geophysics*, **80**(6).

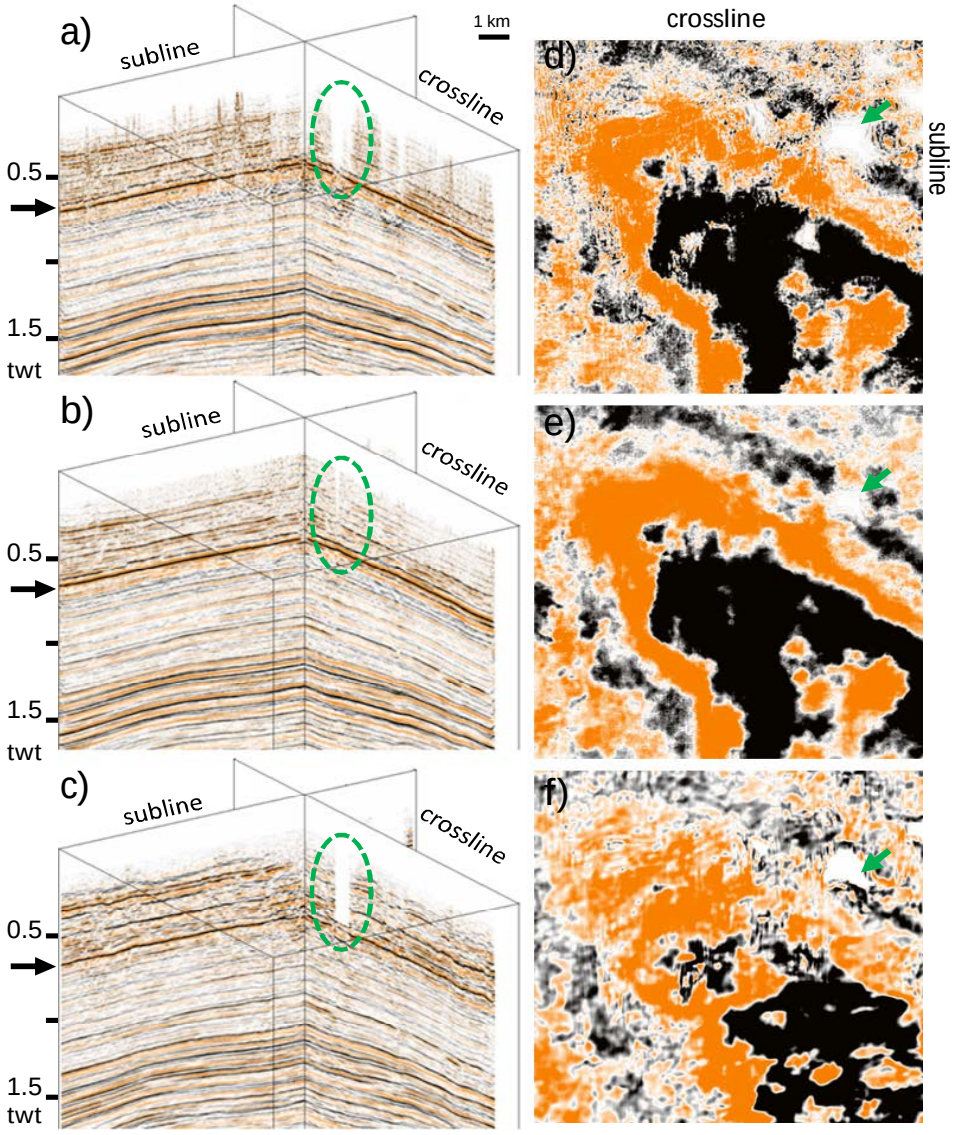

Figure 4 *a) Migrated stack before the 5D regularization, b) Migrated stack after 5D regularization, c) Migrated stack of the vintage data, from d) to f) time-slice at 750 ms.*